Synchrotron X-ray Imaging and Numerical Modelling of Dendritic Sidebranch Evolution during Coarsening

H. Neumann-Heyme[1], N. Shevchenko[1], K. Eckert[1,2], J. Grenzer[1], C. Beckermann[3] and S. Eckert[1]

[1] Helmholtz-Zentrum Dresden-Rossendorf (HZDR), 01314 Dresden, Germany
[2] Institute of Process Engineering, Technische Universität Dresden, 01062 Dresden, Germany
[3] Department of Mechanical and Industrial Engrg., University of Iowa, Iowa City, IA 52242, USA

Abstract

We study the local dynamics of dendritic side arms during coarsening by combining *in-situ* radiography observations with numerical and analytical models. A flat sample of a Ga-In alloy is partially solidified and then held isothermally in a vertical temperature gradient. The evolving dendritic microstructure is visualized by synchrotron X-ray imaging at the BM20 beamline (ESRF, France). The resulting 2D images provide a high resolution in space and time at low noise levels, enabling accurate dynamical measurements. Throughout the initial growth stage there is evidence of solutal natural convection, which however vanishes towards the subsequent coarsening processes. During the coarsening stage, the time evolution of essential geometrical features of side branches was captured by automated image processing. This data is used to quantify the dynamics of three basic evolution scenarios for side branches: retraction, pinch-off and coalescence. We exploit the universal dynamics of sidearm necks during pinch-off to determine the product of liquid diffusivity and capillarity length, Dd_0, as a parameter that is crucial in the calibration of quantitative reference models. By employing an idealized phase-field model for the evolution of a single side branch, we are able to predict the behaviour of selected side branches from the experiment in a consistent way.

Keywords: Dendritic Solidification, Coarsening Dynamics, Material Properties.

1. Introduction

During the last 15 years X-ray imaging techniques have dramatically advanced the in-situ analysis of evolving microstructures in metals [1–3]. Studies have been carried out by radiographic observation of thin samples (2D projections) and to an increasing extent by means of microscopic tomography to obtain time resolved, volumetric data [2]. Radiographic studies in flat samples have addressed various solidification related phenomena depending on composition, cooling rate, gradient magnitude and orientation and the effect of either natural or forced convection conditions.

X-ray micro-tomography provides volumetric information of the microstructure in small bulk samples. The restrictions in terms of sample size and time resolution however remain much more stringent compared to radiography. Therefore, tomography has been mainly useful for the observation of slow processes in small structures e.g. during coarsening of dendrites on a sub-mm scale [3].

Aagesen et al. [4] investigated the isothermal pinch-off of rod-like regions that are part of the coarsening structure embedded in liquid melt. Such structures tend to be prone to a Rayleigh-Plateau like instability mechanism, where a minimum in the cross-section becomes amplified and collapses. When the structure begins to separate, the local curvatures of the neck approach infinity. This strong localization of the neck dynamics causes the process to attain self-similar and universal behaviour when approaching pinch-off. During this stage the geometry of the neck approaches a double cone with an angle of 80 degrees and its diameter evolves as

$$a_N(t) = 1.76\left[Dd_0\left(t_p - t\right)\right]^{1/3} \qquad (1)$$

where D is the solute diffusivity in the liquid phase and d_0 the chemical capillary length.

Neumann-Heyme et al. [5] have recently confirmed in a numerical model, the validity of Eq. (1) just before the detachment of side branches. The numerical study revealed that the pinch-off of side arms can occur only within a limited range of geometrical parameters and cooling rates.

Beyond this parameter interval coalescence or retraction will occur before the side branches can detach from the parent stem. Furthermore, the authors confirmed that the dynamics of the pinching process should correspond to the $t^{1/3}$ - law in the time interval just before pinch-off.

In the present work we perform radiographic analysis on the growth and coarsening of dendrites in a low melting Ga-In alloy at the ROBL beam line (BM20) at the European Synchrotron Radiation Facility (ESRF, Grenoble). Due to the high spatio-temporal resolution, we were able to accurately capture important local geometric features during the coarsening stage, as described above, and to evaluate their dynamics quantitatively. We demonstrate that the measured dynamics can be reproduced very well by means of numerical simulations of an axisymmetric sidearm model, developed in [5].

2. Experimental and modelling procedures

2.1 Experimental setup

The experimental setup used here for the solidification experiments has already been employed for previous radiographic investigations carried out by means of a microfocus X-ray tube [6]. Figure 1 presents a schematic drawing of the solidification cell.
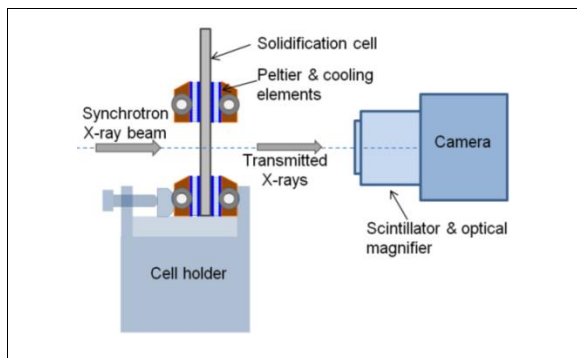

Figure 1: Sketch of the Hele-Shaw solidification cell equipped with arrays of Peltier elements for cooling and heating.

All experiments were conducted in the bottom – up configuration (anti-parallel to gravity) in the low melting temperature Ga–25wt%In alloy, which was prepared from 99.99% Ga and 99.99% In. The low melting point of the alloy (liquidus temperature 15.3 °C) allows for an efficient and flexible implementation of the experiments. Furthermore, the Ga–In alloy exhibits a strong X-ray contrast between the growing Indium dendrites and the interdendritic Ga-rich liquid. The alloy was melted and filled into the Hele-Shaw cell made of Plexiglas with a liquid metal volume of 28 × 28 × 0.15 mm³. The rectangular observation window has a size of 20 × 23 mm². The Hele-Shaw cell was cooled at the bottom by means of a Peltier cooler, while a second array of Peltier elements was mounted on the upper part of the solidification cell as a heater. The distance between the heater and cooler was approximately 19 mm. The simultaneous regulation of the

power of both Peltier elements allows for a flexible control of the cooling rate and the temperature gradient during the process. In the present study a cooling rate of 0.01 K/s and a temperature gradient of -1 K/mm were applied.

The solidification cell was exposed to a monochromatic X-ray beam with energy of 28.5 keV. Conventional transmission radiographs were obtained using a scintillator with a resolution of 2 µm coupled to an optical magnifier and a PCO 2000 CCD camera with 2048 × 2048 pixels. This equipment provides a pixel size of 0.34 × 0.34 µm² and a field of view of about 700 × 700 µm. The distance between detector and sample was approximately 20 cm. Images were acquired at exposure times ranging from 2 to 20 seconds. The exposure times were optimized to achieve an acceptable signal-to-noise ratio and a sufficient contrast for a specific process rate.

2.2 Sidearm model

The quantitative evaluation of sidebranch dynamics in the experiment are complemented by a numerical model to represent a single sidearm that evolves under defined cooling and solutal boundary conditions. The corresponding methodology is described in [5] and incorporates an axisymmetric phase-field model for capillarity-driven interface dynamics in a binary alloy. The present model is based on the assumption of quasi-stationary diffusion as the motion of the interface is slow compared to relaxation of the diffusion field. Hence, temperature is taken as constant and diffusion through the liquid melt only occurs due to curvature differences among distinct regions of the solid-liquid interface.

The initial geometry of the model assumes a pre-existing side branch, which is described by an idealized shape as shown in Figure 2. This geometry captures the essential geometrical characteristics of a simple dendrite side branch, defined by radius, R, length l and having a characteristic lateral spacing λ_r, to its neighbors.
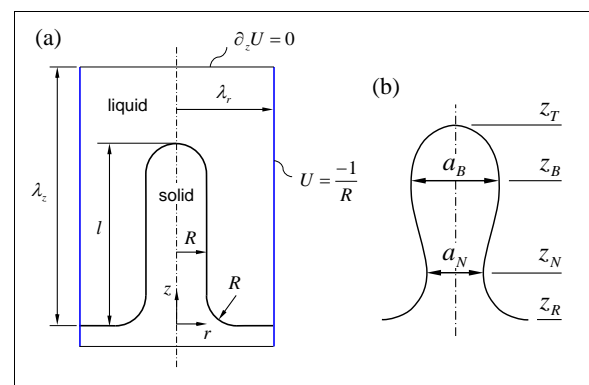

Figure 2: (a) Definitions of model boundaries and initial geometry of the solid and liquid phase. (b) Schematic marking the quantities which are extracted from the synchrotron experiment and simulated by the model (U is the scaled supersaturation).

In contrast to the previous work [5] the radial boundary at $r = \lambda_r$ is defined by a concentration value, which represents an interface of a chosen curvature via the Gibbs-Thomson relation ($1/R$ in the present case). This

allows for modelling a sidearm that is situated between significantly longer arms, such that the tip interacts with the lateral, cylinder-like surfaces of its neighbours. In the present case the neighbour side arms are assumed to have the same radius R as the central arm that is being modelled.

2.3 Material properties of Ga-In

A basic requirement for relating the coarsening model to the actual experiment is the proper specification of the characteristic length scale, here identified as the initial sidearm radius R, and the product of diffusion coefficient and capillary length Dd_0. Whereas $2R$ can be measured directly from the experimental images, the parameter combination Dd_0 is much harder to access.

In the present work we propose a new approach to directly determine the value for Dd_0 from measurements of appropriate dynamical features within the coarsening experiment. For this purpose the experimental data of a pinch-off process are fitted to Eq. (1), as displayed in Figure 5 below, where $Dd_0 = 0.122\ \mu m^3 s^{-1}$ is obtained as a fitting parameter. This value is then used in all subsequent modeling efforts. For comparison, we have calculated a value of $Dd_0 = 0.26\ \mu m^3 s^{-1}$ [11] by evaluating several literature sources [7–9] at the eutectic point, which is close to the present experimental conditions. This value agrees reasonably well with the one from the previous method considering the uncertainties in the various methods and data.

3. Experimental results

The experiments were conducted according to the temperature variations shown in Figure 3. The sample was cooled down over a period of 30 min at a cooling rate of 0.1 K/s. Then, cooling was stopped leading over into an isothermal state which was maintained over a period of 150 min retaining a constant temperature difference of 15°C between heater and cooler. The cooling phase is dominated by dendritic growth whereas dendritic coarsening was observed during the isothermal phase.
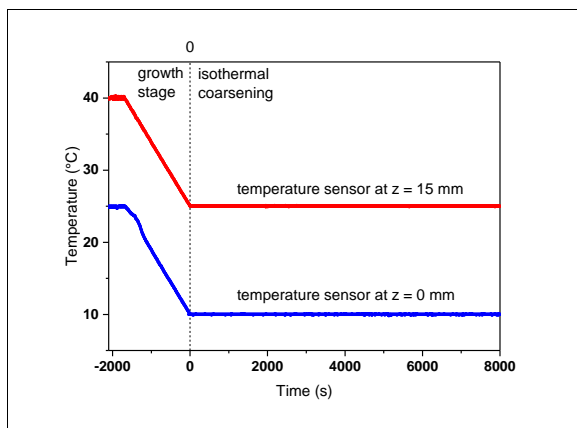

Figure 3: Thermal regime: blue line – temperature near the bottom cooler; red line – temperature near the top heater.

For studying the temporal evolution of the side arm morphology during the isothermal holding stage we selected an observation window which is centered 6.5 mm above the bottom cooler. Figure 4 (a-c) shows an example of the evolution of the shape of the three sidearms (labelled 1, 2, 3) during a pinch-off process. The narrow neck is formed above the junction between the sidearm and the parent stem. Later, the sidearm pinches off at the neck and the resulting fragment coarsens into a spheroid (Fig 4c).
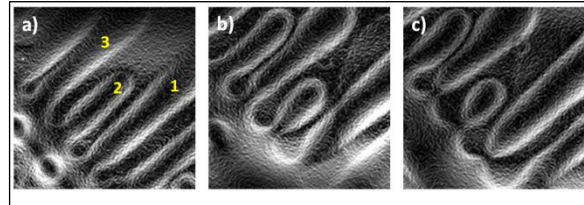

Figure 4: Images showing the development of secondary branches at different time steps in the coarsening state at times (a) $t_p - 5380$ s, (b) $t_p - 1670$ s, and (c) t_p, where the time of pinch-off is $t_p = 7660$ s.

Measured values for the neck diameter as a function of time obtained from image processing are presented in Figure 5. The same behavior of the neck diameter can be observed for all five side arms presented here. It shows the typical dynamics of capillarity-driven pinch-off, where the neck approaches a self-similar state during collapse [4]. The reduction of the neck follows the expected $t^{1/3}$-law. Measurement uncertainties are responsible for the stronger decline of the neck diameter just before the pinch off. Likewise, the scatter of the data is caused by the limited contrast and image noise [11].
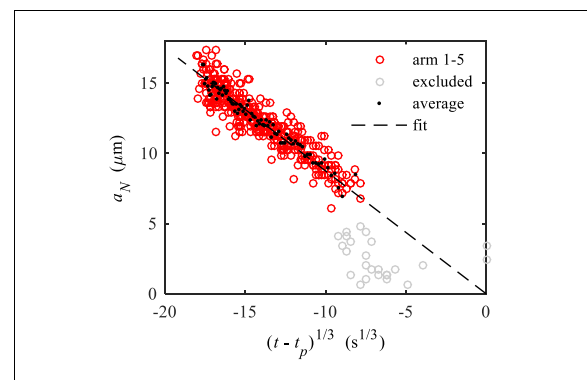

Figure 5: Neck diameter of five individual side arms over non-linear time; dashed line: Eq. (1), where Dd_0 is the fitting parameter.

4. Evaluation and modelling of side arm dynamics

4.1 Modeling results

Figure 6 shows the evolution of the morphological parameters for side arm 2 simulated by using the sidearm model, cf. Figure 2. The numerical results (black lines) are compared here with the corresponding measurements (red circles).
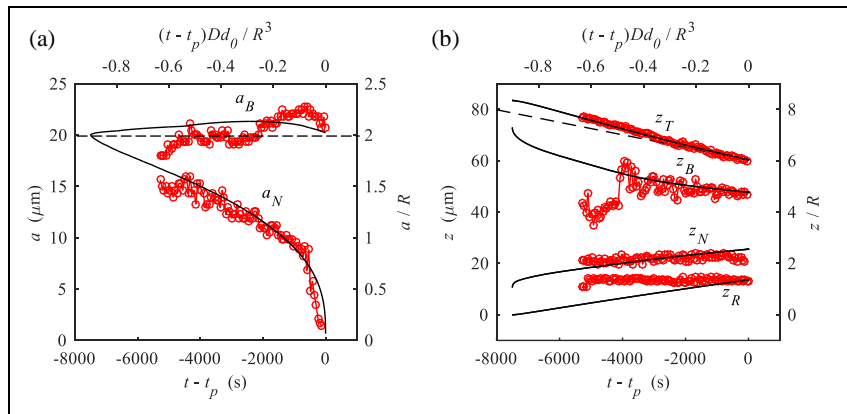
Figure 6: Evolution of morphological parameters for side arm 2; red circles: experimental measurements, black lines: numerical model; bottom and left axes are in physical units, top and right axes in scaled units, respectively; (a) bulge and neck diameter, dashed line: reference for initial radius $R = a/2$; (b) vertical positions for tip, bulge, neck and root; dashed line: analytical model [10]. The variables plotted were introduced in Figure 2.

Under isothermal coarsening conditions, where the overall volume of solid material is conserved, the observed melting and deposition processes can be interpreted as a transfer of solid from regions of higher to lower mean curvature. Retraction of the tip is governed by its comparably higher curvature with respect to the adjacent interface regions of the neighbor side arms. The circumstance that the relevant curvatures and other geometrical properties remain essentially unchanged is reflected by the linear decrease of the longitudinal tip coordinate z_T in Figure 6b. For comparison, the result of a simple retraction model [10] for similar conditions is shown by a dashed line,

In parallel with retraction of the sidearm tip, a narrowing of the neck takes place, where the sidearm is connected to its parent stem. This remelting process is driven by the contrast between the increasing curvature of the neck and the nearby root region of low curvature. It leads into accelerated pinching and detachment of a sidearm fragment, as seen from the dynamics of the neck diameter a_N in Figure 8a. Subsequently, the resulting fragment is typically carried away by buoyant action and may re-attach to the solid structure, undergo further coarsening or may continue growing as an equiaxed dendrite in the undercooled melt.

During the entire process, the longitudinal position of the neck z_N remains practically unchanged with respect to the root coordinate z_R. The position of the bulge z_B behaves in an intermediate way between z_N and z_T, however being affected by a high uncertainty at earlier times, where a clear maximum in the arm diameter has not yet developed. The bulge diameter a_B remains roughly constant, although a slight increase appears towards the end, which can be attributed to a growing of the bulge when approaching the remelting necks of the neighbor branches.

5. Conclusions

The isothermal coarsening of the dendritic microstructure in a Ga-In alloy was studied by means of a numerical model for the development of dendrite side arms and synchrotron X-ray imaging. The X-ray diagnostic technique enables for visualizing the temporal evolution of the side arm with high spatial resolution, thereby enabling measurements of relevant geometrical parameters such as side arm length or neck diameter [11].

For the isothermal stage, the X-ray experiment has shown two dominant scenarios for morphological transitions of the sidearms: retraction and pinch-off. We demonstrate that the measured dynamics can be reproduced very well by means of numerical simulations of an axisymmetric side arm model. The corresponding temporal dynamics of the pinching processes have been utilized to the determination of the parameter Dd_0, which is a parameter of primary interest in modelling solidification and coarsening processes. This procedure has the potential to quantify the value for Dd_0 by in-situ observation followed by a rather simple theoretical analysis, which otherwise needs to be acquired from various delicate experiments.

Acknowledgements

References

1. R. H. Mathiesen et al., *Phys Rev Lett*, 1999, **83**: 5062.
2. H. Nguyen-Thi et al., *C R Phys*, 2012, **13**:237.
3. N. Limodin et al., *Acta Mater*, 2009, 2300.
4. L.K. Aagesen et al., *Acta Mater*, 2011, 59, 4922.
5. H. Neumann-Heyme et al., *Phys Rev E*, 2015, **92**: 060401.
6. N. Shevchenko, *Metall Mater Trans A*, 2013, 44: 3797.
7. W.F. Gale and T.C. Totemeier, *Smithells Metals Reference Book* (Butterworth-Heinemann, 2003).
8. W. Tyson et al., *Surf Sci*, **62**, 267 (1977).
9. P.A. Savintsev et al., *Sov Phys J*, 53 (1971).
10. M. Chen et al., *Mat Sci Eng −Struct*, **247**, 239 (1998).
11. H. Neumann-Heyme et al. (in preparation).

SP17

Solidification Processing 2017

Proceedings of the
**6th Decennial
International Conference on
Solidification Processing**

25 - 28 July 2017
Beaumont Estate
Old Windsor, UK

Edited by Z. Fan

BCAST